European Journal of Oral Sciences

Eur J Oral Sci 2014; 122: 382–390
DOI: 10.1111/eos.12151

European Journal of Oral Sciences

Nuclear factor I-C expression pattern in developing teeth and its important role in odontogenic differentiation of human molar stem cells from the apical papilla

Shuo Gao, Yu-Ming Zhao, Li-Hong Ge

Department of Pediatric Dentistry, Peking University School and Hospital of Stomatology, Peking University Health Science Center, Peking University, Beijing, China

Gao S, Zhao Y-M, Ge L-H. Nuclear factor I-C expression pattern in developing teeth and its important role in odontogenic differentiation of human molar stem cells from the apical papilla.
Eur J Oral Sci 2014; 122: 382–390. © 2014 Eur J Oral Sci

Nuclear factor I-C (NFIC) has an important role in the development of murine dental roots, but its role in human root formation is unreported. We thus elucidated the regulatory role of NFIC in the differentiation of human stem cells from the apical papilla (hSCAPs). The first step for this was to determine the expression of NFIC in human teeth, and it was found that NFIC expression was restricted to the odontoblasts and preodontoblasts of the developing molars of humans and mice. NFIC was found to be expressed in odontoblast-like cells after the subcutaneous transplantation of hSCAPs. NFIC expression was concomitant with dentin sialophosphoprotein (DSPP) in the mineralization of hSCAPs. NFIC knockdown in hSCAPs significantly inhibited expression of *DSPP* and promoted that of dentin matrix protein 1 (*DMP1*), meanwhile upregulated the expression of *TGF-β1* and downregulated *SMAD3* and *SMAD4*. NFIC expression was significantly upregulated after *TGF-β1* treatment in hSCAPs. NFIC knockdown prolonged G1 phase of the cell cycle, but had no effect on cell proliferation and migration. These results suggest that NFIC is involved in the development of human root dentin and the regulation of odontoblastic differentiation of hSCAPs. NFIC may participate in the DMP1-DSPP signaling pathway and comprises a complex signaling cycle with TGF-β1.

Dr Li-Hong Ge, Department of Pediatric Dentistry, Peking University School and Hospital of Stomatology, Peking University Health Science Center, Peking University, #22 Zhongguancun Nandajie, Haidian District, Beijing 100081, China

E-mail: gelh0919@126.com

Key words: dental root development; hSCAPs; human; NFIC; odontogenic differentiation

Accepted for publication August 2014

The formation of a dental root is the result of the interaction between the epithelial root sheath, dental papilla and dental follicle. Dental ectomesenchymal cells from the dental papilla differentiate into odontoblasts to produce a dentin layer that forms the bulk of the tooth. However, the molecular mechanisms underlying ectomesenchymal cells differentiation into odontoblast are not well understood.

The nuclear factor I (NFI) family of transcription-replication factors (1) encodes four members (*Nfia*, *Nfib*, *Nfic*, *Nfix*) in mammals, which are expressed in almost every tissue and organ (2). However, mice with disruptions in each of the *NFI* genes have been found to display distinct phenotypes and developmental defects primarily in the nervous system (*Nfia*) (3), lung and brain (*Nfib*) (4, 5), and brain and skeleton (*Nfix*) (6), indicating different functions for each NFI subtype. Specifically, loss of *Nfic* is the first mouse mutation to affect the development of dental roots. Studies have demonstrated that *Nfic* null mice exhibit abnormal roots of molar teeth containing aberrant odontoblasts and abnormal formation of dentin, but normal crowns. NFIC should be necessary for root development (7, 8). However, the mechanism by which disruption of the *Nfic* gene leads to abnormal root formation remains unclear. Also, the relationship between NFIC and the formation of human dental roots has not been reported.

The transforming growth factor (TGF)-β superfamily have wide-ranging functions in the proliferation and differentiation of cells, the epithelial-to-mesenchymal transition, embryonic development as well as several biologic processes (9). TGF-β1 has been implicated to have an important role in regulating odontoblast differentiation in murine tooth development (10). Some evidences support the interaction between NFIC and TGF-β signaling. Expression of TGF-β1 and TGF-β3 is upregulated in *Nfic*-deficient incisor primary pulp cells (11). Conditional overexpression of TGF-β1 in mouse odontoblasts displays the same phenotypic dysplasia as that seen in $Nfic^{-/-}$ mice (12). However, the exact mechanism behind the interaction between NFIC and TGF-β1 signaling is not known.

In the present study, we focused on the root development of human molars and the differentiation of stem cells from the apical papilla (SCAPs). We sought to determine NFIC expression in young permanent human teeth and in the mineralization of human SCAPs. Furthermore, we investigated if knockdown of the NFIC gene causes biological changes in hSCAPs. We also tested the hypothesis that the homeostatic interaction between NFI-C and TGF-β1 signaling regulates the differentiation of stem cells into odontoblasts.

Material and methods

The procedure to obtain healthy extracted teeth was approved by the Ethical Committee of the Health Science Center of Peking University (Beijing, China) (IRB00001052-11060). Patients provided written informed consent. Normal human impacted third molars with open apical foramina and closed apical foramina were collected at a clinic in Peking University School and Hospital of Stomatology.

C57BL/6J mice were obtained from the Experimental Animal Department of Peking University Health Science Center. Care and the handling of animals was in accordance with Institutional and National guidelines. This study was approved by the Animal Ethics Committee of Peking University (LA2012-58). Mice were decapitated while under anesthesia and then first molars were isolated at postnatal day 1–20 (P1–P20).

Cell culture, induction of mineralization and TGF-β1 stimulation

Apical papilla tissues separated gently from the end of human teeth were digested in a solution of 3 mg ml^{-1} collagenase type I (Sigma-Aldrich, Basel, Switzerland) and 4 mg ml^{-1} dispase (Sigma-Aldrich) for 1 h at 37°C. Cultures were maintained in α-modified Eagle's minimum essential medium (α-MEM; Gibco, Grand Island, NY, USA) supplemented with 10% fetal bovine serum (FBS; Hyclone, Logan, UT, USA) in 5% carbon dioxide at 37°C. The cells used were at passages 1–4. For each experiment, the same passage of hSCAPs was used.

Seventy to eighty percent confluent hSCAPs were cultured in differentiation medium supplemented with 10% FBS, 10 mM β-glycerolphosphate, 50 mg ml^{-1} ascorbate phosphate, 10 nM dexamethasone, and 10 nM 1,25-dihydroxyvitamin D3 for 3 over wk. The medium was changed every 3 d thereafter. Cultures were fixed in 4% paraformaldehyde. Calcium deposition of the extracellular matrix was evaluated by staining with 1% alizarin red-S (Sigma-Aldrich).

When cells had grown to 70–80% confluence, hSCAPs were simulated with TGF-β1 (5 ng ml^{-1}; PeproTech, Rocky Hill, NJ, USA) for 24 h at 37°C.

Transplantation

Approximately 2.0×10^6 in vitro-expanded hSCAPs mixed with 40 mg hydroxyapatite ceramic particles (Bio Osteon, Beijing, China) were transplanted subcutaneously into the dorsal surfaces of 10-wk-old immunodeficient mice (CB-17/SCID; Vitalriver, Beijing, China) according to a method reported previously (13). A cell-free group served as a negative control. Transplants were harvested 8 wk after transplantation.

Immunocytochemistry

Samples were fixed in 4% paraformaldehyde, then decalcified in 10% EDTA and processed for embedding in paraffin. Immunohistochemical staining was undertaken on 4 μm-thick tissue sections, which were deparaffinized with xylene and rehydrated with descending concentrations of ethanol, then quenched endogenous peroxidase activity by treatment with 3% H_2O_2 for 10 min at room temperature. Antigen retrieval was achieved by 1 mg ml^{-1} trypsin digestion at 37°C for 10 min. Sections were incubated with mouse anti-NFIC primary antibody (1:400 dilution; Abcam, Cambridge, UK) diluted in antibody diluent (Zhongshan Golden Bridge Biotechnology, Beijing, China) at 4°C overnight. After being washed with phosphate-buffered saline (PBS, 0.01 M, pH 7.4), the location of NFIC was visualized by using a Polymer Detection System for IHC Staining kit and a 3,3′-diaminobenzidine (DAB) kit (Zhongshan Golden Bridge Biotechnology). Sections were finally counterstained with hematoxylin and mounted. The specificity of the immunoreaction was confirmed by incubation with normal mouse IgG (Santa Cruz, CA, USA) and a preadsorption experiment. Images were captured on a digital microscopic system (BX51/DP72; Olympus, Tokyo, Japan).

The same passage of hSCAPs was subcultured onto 24-chamber slides (4×10^4/well, third passage) and grown to 80% confluence. The same passage of hSCAPs grown to 80% confluence on slides were immunocytochemically stained as described above.

Transfection

Before transfection, the medium was replaced with antibiotic-free medium. To detect the efficiency of small interfering ribonucleic acid (siRNA) transfection, green fluorescent control siRNA (BLOCK-iT Fluorescent Control; Invitrogen, Carlsbad, CA, USA) was transfected into hSCAPs using Lipofectamine 2000 Transfection Reagent (Invitrogen).

The nucleotide sequences of the special-labeled *NFIC* siRNA were: 5′-GGAAGCGCAAGUACUUCAAdTdT-3′ (sense),3′-dTdTCCUUCGCGUUCAUGAAGUU-5′ (antisense) (RiboBio, Guangzhou, China). NFIC knockdown was achieved through transfection with RNA interference (RNAi) Lipofectamine 2000 Transfection Reagent according to manufacturer's instructions, whereas the cells transfected with Stealth RNAi siRNA Negative Control Med GC (Invitrogen) were served as the negative control group. When the cells had grown to 30–40% confluence, we proceeded with transfection by diluting Lipofectamine 2000 in Opti-MEM I Medium (Invitrogen) without serum in a RNase-free centrifuge tube and incubating for 5 min at room temperature, and diluting siRNA in Opti-MEM I Medium (100 nM). Diluted Lipofectamine 2000 and diluted RNAi molecules were mixed gently and incubated for 20 min at room temperature to allow complex formation to occur. Finally, RNAi duplex-Lipofectamine 2000 complexes were added to the cell culture and incubated at 37°C in a carbon-dioxide incubator.

RT-PCR analysis

Total RNA was extracted using TRIzol Reagent (Invitrogen) according to the manufacturer's instructions. cDNA was synthesized using an AMV Reverse Transcriptase kit (Fermentas, St. Leon-Rot, Germany). The primer sequences used were designed and tested using a basic local alignment search tool (BLAST) (Table 1). Polymerase chain reactions (PCR) was carried out in triplicate in 96-well plates using a 7900HT Fast Real-time system (Applied Biosystems, Carlsbad, CA, USA). The reaction mix contained 1.0 μl of pre-amplified cDNA, 400 nM of primers, 10 μl of Power SYBR Green PCR Master Mix (Roche, Basel, Switzerland) and DEPC-water to complete a final volume of 20 μl. Melting curves at the final stage were used to verify the specificity of each primer pair. The comparative cycle threshold ($\Delta\Delta C_T$) method was used to calculate the relative levels of expression of the target gene.

Table 1

Primer sequences for RT-PCR

Gene	Primer sequence
GAPDH	Forward 5′-GGAGCGAGATCCCTCCAAAAT-3′
	Reverse 5′-GGCTGTTGTCATACTTCTCATGG-3′
NFIC	Forward 5′-ACCTGGCATACGACCTGAAC-3′
	Reverse 5′-TCCATCGAGCCCGATTTGTG-3′
DSPP	Forward 5′-TGGCGATGCAGGTCACAAT-3′
	Reverse 5′-CCATTCCCACTAGGACTCCCA-3′
DMP1	Forward 5′-CACTCAAGATTCAGGTGGCAG-3′
	Reverse 5′-TCTGAGATGCGAGACTTCCTAAA-3′
ALP	Forward 5′-ATGGGATGGGTGTCTCCACA-3′
	Reverse 5′-CCACGAAGGGGAACTTGTC-3′
OCN	Forward 5′-CACTCCTCGCCCTATTGGC-3′
	Reverse 5′-CCCTCCTGCTTGGACACAAAG-3′
COL1A 1	Forward 5′-GTGCGATGACGTGATCTGTGA-3′
	Reverse 5′-CGGTGGTTTCTTGGTCGGT-3′
TGF-β1	Forward 5′-CAATTCCTGGCGATACCTCAG-3′
	Reverse 5′-GCACAACTCCGGTGACATCAA-3′
TGF-β-RI	Forward 5′-CACAGAGTGGGAACAAAAAGGT-3′
	Reverse 5′-CCAATGGAACATCGTCGAGCA-3′
SMAD2	Forward 5′-CGTCCATCTTGCCATTCACG-3′
	Reverse 5′-CTCAAGCTCATCTAATCGTCCTG-3′
SMAD3	Forward 5′-CCATCTCCTACTACGAGCTGAA-3′
	Reverse 5′-CACTGCTGCATTCCTGTTGAC-3′
SMAD4	Forward 5′-CCACCAAGTAATCGTGCATCG-3′
	Reverse 5′-TGGTAGCATTAGACTCAGATGGG-3′
Cyclin D1	Forward 5′-TGGAGCCCGTGAAAAAGAGC-3′
	Reverse 5′-TCTCCTTCATCTTAGAGGCCAC-3′
CDK4	Forward 5′-ATGGCTACCTCTCGATATGAGC-3′
	Reverse 5′-CATTGGGGACTCTCACACTCT-3′
Cyclin E	Forward 5′-GCCAGCCTTGGGACAATAATG-3′
	Reverse 5′-CTTGCACGTTGAGTTTGGGT-3′
Cyclin A	Forward 5′-TAGACACCGGCACACTCAAG-3′
	Reverse 5′-AGGAGAGATGAATCTACCAGCAT-3′
CDK2	Forward 5′-CCAGGAGTTACTTCTATGCCTGA-3′
	Reverse 5′-TTCATCCAGGGGAGGTACAAC-3′
Cyclin B1	Forward 5′-AATAAGGCGAAGATCAACATGGC-3′
	Reverse 5′-TTTGTTACCAATGTCCCCAAGAG-3′

GAPDH, glyceraldehyde-3-phosphate dehydrogenase; *NFIC*, nuclear factor I-C; *DSPP*, dentin sialophosphoprotein; *DMP1*, dentin matrix protein 1; *ALP*, alkaline phosphatase; *OCN*, osteocalcin; *COLLA I*, collagen type I; *TGF-β1*, transforming growth factor-β 1; *TGF-β-RI*, TGF-β receptor I; *SMAD*, SMAD family member; *CDK*, cyclin-dependent kinase.

Western blotting

Total protein was extracted using a radioimmunoprecipitation assay buffer (RIPA) containing a protease inhibitor cocktail (Applygen, Beijing, China). Protein levels were detected using a BCA Assay kit (Thermo Scientific, Waltham, MA, USA). Proteins (30 μg) were separated by sodium dodecyl sulfate – polyacrylamide gel electrophoresis (SDS-PAGE) and transferred onto a polyvinylidene fluoride membrane. After blocking with 5% (w/v) non-fat dried milk, the membrane was incubated overnight at 4°C with primary antibodies against NFIC (Abcam) and dentin sialoprotein (DSP; Santa Cruz) and GAPDH (Abmart, Shanghai, China). Blots were then reacted with a horseradish-peroxidase-conjugated secondary antibody (Origene, Beijing, China) and visualized by enhanced chemiluminescence (Applygen) at room temperature.

Cell-proliferation assays

The proliferation of hSCAPs after transfection was assessed using a Cell-Light 5-ethynyl-2′-deoxyuridine (EdU) Imaging Detection kit (Ribo-Bio, Guangzhou, China) and a Cell Counting Kit-8 (Dojindo Laboratory, Kumamoto, Japan) at 24, 48, and 72 h, according to the manufacturer's instructions.

Cell-cycle assay by flow cytometry

Cells were harvested after transfection for 48 h and fixed in ice-cold 70% ethanol for at least 12 h. After washed with PBS twice, samples were incubated with RNase A, DNase, and protease-free solutions (Fermentas) for 30 min to remove RNA, and then stained with 50 μg ml^{-1} propidium iodide (PI). DNA analysis was performed in an EPICS RL flow cytometer (Beckmann Coulter, Hialeah, FL, USA) with COULTER EPICS SYSTEM IITM software.

Wound-healing assay

hSCAPs were plated in 12-well dishes and treated with siRNA as described above. After transfection for 6–8 h, the medium was changed into α-MEM containing 1% FBS. Wounds were made using a pipette tip and photographs taken immediately (time 0) and 24, 48 and 72 h after wounding. The numbers of cells migrating into the wounded area during this time period was measured. Experiments were carried out in triplicate and repeated at least five times.

Statistical analyses

Statistical analysis was performed using SPSS software, version 15.0 (SPSS, Chicago, IL, USA). A P-value of <0.05 was considered to indicate a statistically significant difference between experimental groups. Student's t-test and chi-square test was used to analyze differences between groups. All experiments were repeated at least three times.

Results

NFIC expression in tooth tissue and transplanted hSCAPs

To determine the expression pattern of NFIC during the formation of molar roots, we conducted

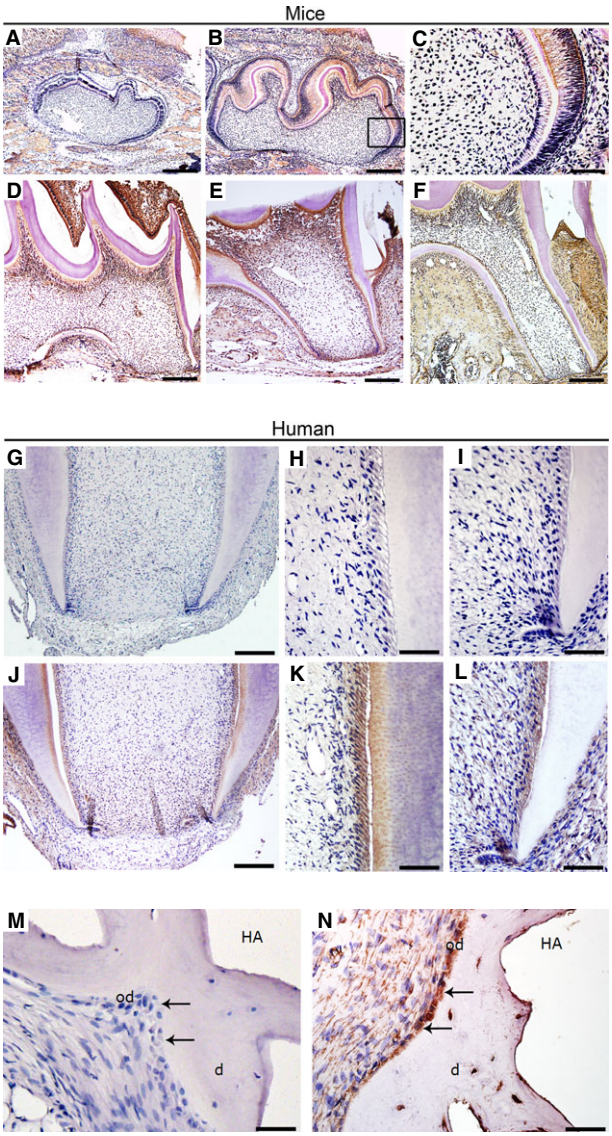

Fig. 1. NFIC expression in tooth tissue and the transplantation of hSCAPs. (A, B) Immunohistochemical analyses showing NFIC expression in the developing crown of P1 and P3 murine first mandibular molar. (C) Higher magnification of the boxed area in B. (D, E, F) NFIC immunoreactivity in the murine developing tooth at P10, P15 and P20 respectively. (G, H, I) Control staining showing the developing root of human young permanent third molar. (J, K, L) NFIC immunoreactivity in the same areas of G, H, I. (M) Control staining and (N) immunohistochemical straining of NFIC in a dentin–pulp–like complex ex vivo 8 wk after transplantation of hSCAPs into the dorsum of immunocomprized mice (*arrows* odontoblast-like cells lining the surfaces of dentin-like structures surrounding pulp-like tissue; d, dentin-like structures; od, odontoblast-like cells; HA, hydroxyapatite). Scale bars 200 μm (A, B, D–G, H), 50 μm (C, H, I, K–N).

immunohistochemical staining for the molar roots of mice and humans. In developing crown of murine molars, NFIC was expressed in odontoblasts and ameloblasts (Fig. 1A–C). When root formation was in progress, NFIC was expressed strongly in odontoblasts and preodontoblasts, moderately in periodontal ligaments

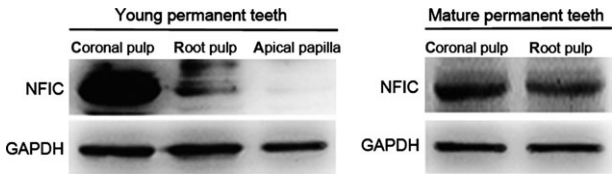

Fig. 2. Quantification of NFIC expression in the coronal pulp, root pulp and apical papilla of human tooth by western blotting.

and alveolar bone yet weakly in the pulp and apical papilla (Fig. 1D–F). During root development of human young permanent tooth, NFIC expression was restricted within odontoblasts and preodontoblasts and weakly within the pulp and apical papilla. No immunohistochemical staining was seen in Hertwig's epithelial root sheath (HERS) (Fig. 1G–L).

To study the expression of NFIC during odontoblast differentiation ex vivo, hSCAPs with hydroxyapatite carriers were transplanted into immunocompromised mice. Eight weeks after transplantation, the hSCAPs generated dentin-like structures. Odontoblast-like cells aligned in a layer along the surface of dentin-like structures were positive to NFIC immunohistochemical straining (Fig. 1M,N).

NFIC expression in different parts of human dental pulp was quantified. NFIC was expressed in the apical papilla at a very low level, and the amounts of NFIC protein in the coronal pulp were more than that in the root pulp in young and mature permanent teeth. NFIC expression in the coronal pulp of young permanent teeth was extremely strong (Fig. 2).

NFIC expression in induced mineralization of hSCAPs

To determine how NFIC was expressed if hSCAPs differentiated in vitro, cells were cultured in mineralization medium for about 3 wk and expression of markers of odontoblast differentiation and dentin mineralization analyzed by western blotting and RT-PCR. Alizarin red-S staining revealed the presence of red mineralized nodules from d6 after the induction of differentiation (Fig. 3A). NFIC protein expression had a fluctuating trend before d15 and then decreased, and the expression of DSP showed a similar pattern to that of NFIC according to western blotting (Fig. 3B) and RT-PCR. The mRNA expression levels of alkaline phosphatase (*ALP*) and osteocalcin (*OCN*) increased significantly from d12 and continued to increase to d25 ($P < 0.05$) (Fig. 3C). Based on these findings, we concluded that the expression pattern of NFIC and DSP were similar during the mineralization of hSCAPs in vitro.

Transfection and knockdown efficiency

As shown in Fig. 4A, green fluorescent control siRNA was efficiently delivered into almost all the hSCAPs (~92%). Therefore, Lipofectamine 2000 was considered an ideal tool for delivering siRNA into the hSCAPs.

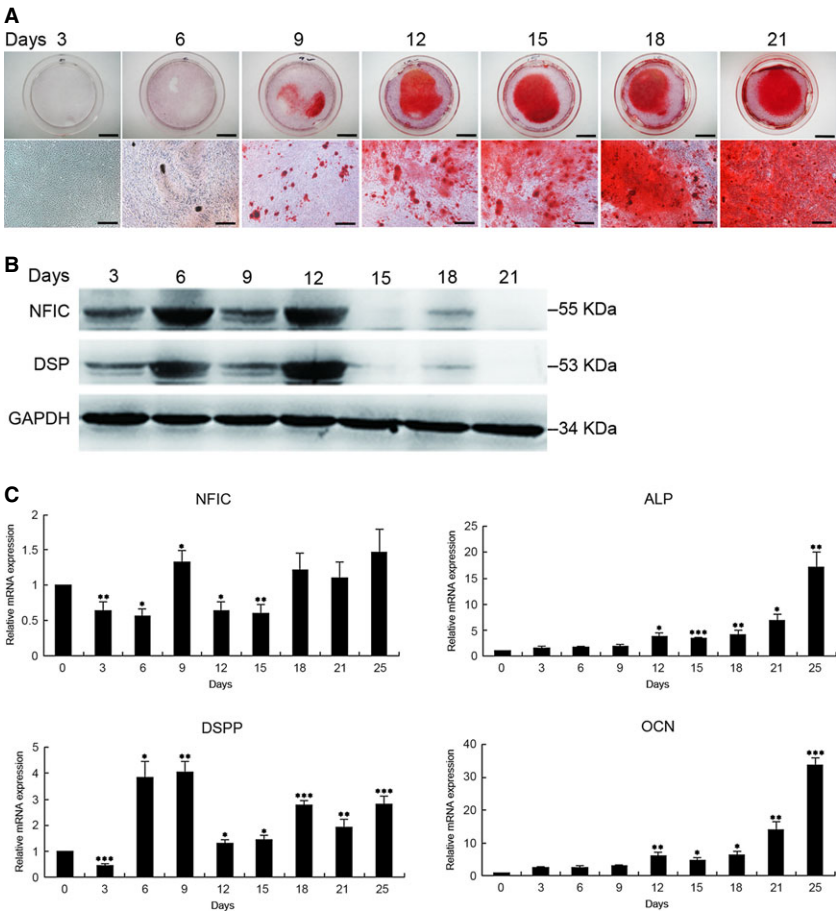

Fig. 3. NFIC expression in induced mineralization of hSCAPs. After the induction of osteogenic differentiation (A) Alizarin red-S staining shows formation of mineralized nodules, Scale bars 10 mm (above), 500 μm (below) (B) expression of NFIC and DSP was evaluated by western blotting and (C) expression of *NFIC*, *DSPP*, *ALP* and *OCN* was evaluated by RT-PCR.*$P < 0.05$, **$P < 0.01$ and ***$P < 0.001$. *GAPDH* was used as a loading control.

The following RT-PCR and Western blooting experiment demonstrated that the mRNA (Fig. 4B) and protein (Fig. 4C) levels of NFIC decreased sharply at 24, 48 h respectively after transfection with NFIC siRNA.

NFIC knockdown does not affect proliferation and migration but prolongs the G1 phase of hSCAPs

To determine the effect of NFIC knockdown on hSCAPs proliferation, EdU (Fig. 5A) and CCK-8 assays were used at 24, 48, and 72 h. For each time point the mean percentage representing the proportion of proliferating hSCAPs (Fig. 5B) and the mean absorbance values representing the cells viability (Fig. 5C) are shown. We found that the differences of the hSCAPs proliferation observed between the NFIC siRNA group and the control group have no sense in statistics. These results indicate that NFIC might have no effect on hSCAPs proliferation under physiological conditions.

The effect of NFIC knockdown on the cell cycle distribution of hSCAPs was examined. Flow cytometry analysis demonstrated that NFIC knockdown induced an increase of cells in G0/G1 phase from 57.0% to 65.8%, indicating G1 cell cycle arrest compared with the control group (Fig. 5D). Furthermore, the mRNA expression levels of the G1-phase-related genes Cyclin E and G2-phase-related genes Cyclin B1, were significantly reduced in the NFIC siRNA group compared with the control group (Fig. 5E). Taken together, these results suggest that NFIC knockdown leads to G1-phase arrest of hSCAPs and that NFIC may participate in regulating cell cycle progression.

In wound-healing assays, the distance moved by a wounded cell monolayer on plastic after transfection was obtained (Fig. 5F). The results reported as the numbers of cells migrating into the distance to close the wound showed that there was no significant difference in hSCAPs migration between the two groups until the cells achieve wound closure at 72 h (Fig. 5G).

Knockdown of NFIC inhibits the expression of DSPP

The effect of *NFIC* knockdown on the expression of the related genes of odontoblast differentiation of hSCAPS was studied. RT-PCR revealed that the

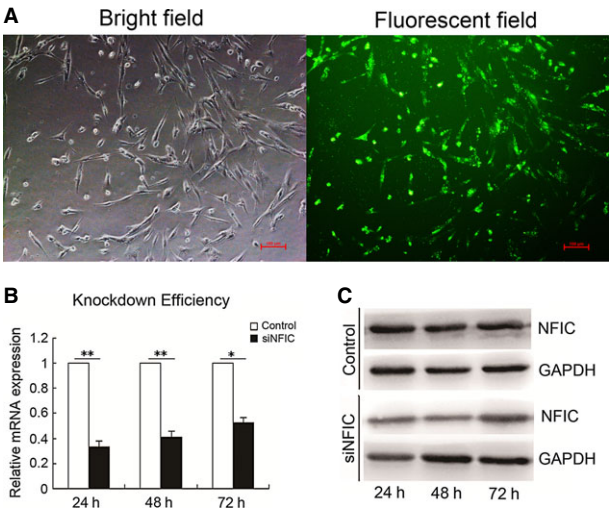

Fig. 4. Transfection efficiency of siRNA and *NFIC* knockdown efficiency. (A) Representative photographs of transfected hSCAPs with green fluorescent control siRNA. Quantification of NFIC knockdown at mRNA (B) and protein (C) levels is shown 24 h 48 h and 72 h, after transfection with control and NFIC siRNAs. Knockdown efficiency at 24 h is 33.25% at the mRNA level. *GAPDH*, glyceraldehyde-3-phosphate dehydrogenase. $^{**}P < 0.01$.

expression levels of the marker of odontoblast differentiation (*DSPP*) was decreased significantly in the *NFIC* siRNA group compared with the control group. Yet the expression of *DMP1* was increased significantly. Expression of *ALP*, *OCN* and collagen type I (*COL1A 1*) was not significantly changed (Fig. 5H). *NFIC* downregulation significantly inhibited the expression of *DSPP* and promoted that of *DMP1*.

Interaction of NFIC with TGF-β1

TGF-β1-overexpressing transgenic mice have similar dentin dysplasia to that seen in *Nfic*-deficient mice (11). *Nfic*-deficient mice have higher levels of TGF-β-R1 and p-Smad2/3 in the odontoblasts and pulp cells of their incisors (10). Therefore, we next measured the effect of TGF-β1 treatment on the level of endogenous NFIC protein in hSCAPs to investigate the relationship between NFIC and TGF-β1 signaling in vitro. NFIC was upregulated after TGF-β1 addition in hSCAPs according to immunocytochemical straining (Fig. 6A) and western blotting (Fig. 6B). Additionally, expression levels of *TGF-β1* were increased significantly compared with the control group but *SMAD3* and *SMAD4* were decreased significantly. *NFIC* downregulation significantly inhibited the expression of *SMAD3* and *SMAD4*, and promoted that of TGF-β1 (Fig. 6C).

Discussion

Studies have shown that disruption of *Nfic* can cause major defects in postnatal tooth development in mice, with the most striking defect being loss of formation of molar roots. In general, it is thought that NFIC is one of the molecules required for root formation. However, most authors have made conclusions based on experiments with non-molar root tissues (e.g. jaw, incisor) or murine cell lines (7, 8, 14–17). Mice mirror, to a certain extent, what happens in humans, but they are not perfect model animals. To further explore the function of NFIC on human root development, we used hSCAPs, which can differentiate into odontoblasts located in roots to generate root dentin.

In this study, we found that in the developing crown of murine molars, NFIC was expressed in ameloblasts and odontoblasts. The possible explanation of normal enamel formation in *Nfic* null mice could be that NFIC may be involved in ameloblast differentiation or the interactive induced differentiation of ameloblasts and odontoblasts, but not a key regulator of this process.

In tooth root tissue of human young molar, NFIC expression appeared most strongly within odontoblasts and preodontoblasts, though it could also be seen in the periodontal ligament, and very weakly in the pulp and the apical papilla. No NFIC expression was detected in HERS. Thus the expression of NFIC in human tooth show the similar distribution to mice, which was concentrated in the odontoblast layer directly related to dentin formation, but not observed obviously in HERS as a key role in the induction of EM differentiation at the start of root development, suggesting that NFIC exert effects on human odontogenic differentiation and dentin formation. Moreover, the level of NFIC protein in young permanent teeth was higher than that seen in mature permanent teeth, as well as very low in apical papilla. Therefore, we speculated that the expression level of NFIC was positively correlated with the differential degree of odontoblasts. Thus the young permanent teeth in the active period of dentin formation expressed higher level of NFIC than mature teeth, and NFIC is rarely expressed in apical papilla tissue not yet entering into odontoblastic differentiation. Considering *Nfic*$^{-/-}$ mice developed abnormal root but normal crown, our results that NFIC expression was higher in the coronal pulp than in the root pulp suggesting that the mechanisms of odontogenesis might be different in the coronal pulp and root pulp, which required further studies.

It is well established that the HERS regulates the formation of organized root dentin through epithelial-mesenchymal interactions. The absence of the HERS during the formation of secondary or reparative dentin would attenuate the ability of odontoblast progenitor cells to form organized advancing dentin and would cause them to form osteodentin without organized dentinal tubules structure instead (18). In this study when hSCAPs were transplanted into the dorsum of immunocompromized mice and a dentin-like structure was generated, NFIC was expressed in odontoblast-like cells in osteodentin that resembled repair dentin, which conceivably imply that NFIC participates in the hSCAPs differentation ex vivo and the generation of osteodentin. The mechanisms behind the osteodentin formation and odontoblast-like cells differentiation remain

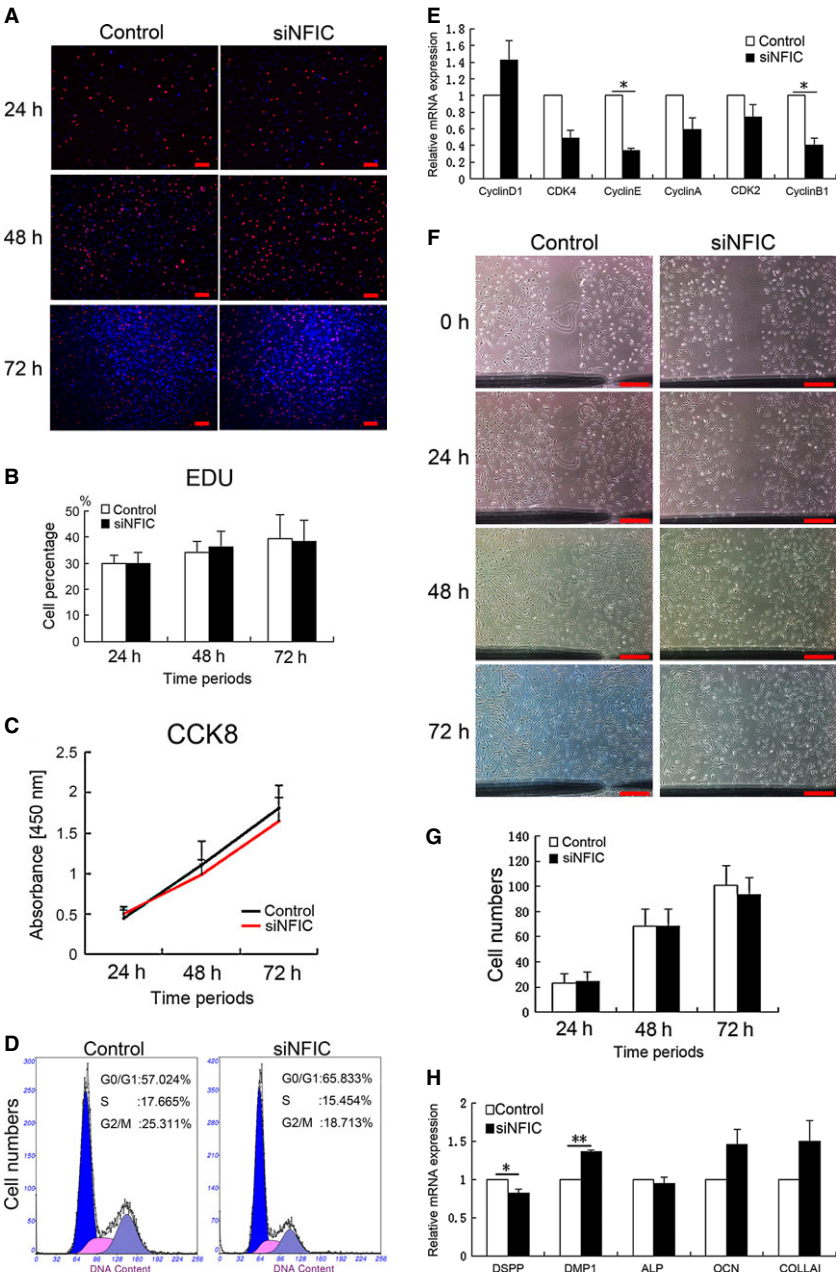

Fig. 5. Effects of NFIC knockdown on the proliferation, cell cycle, migration and the expression of related odontoblastic genes of hSCAPs. (A) Representative photographs of negative control and NFIC siRNA-transfected cells, 24, 48, and 72 h after transfection, are shown following incorporation of EdU to assess cell proliferation. Red, EdU-positive cells; Blue, Hoescht-stained cells. (B) Quantification of the rate of cell proliferation are plotted 24, 48, and 72 h after transfection. At each time point the rate of cell proliferation in the control group was 30.05%, 34.16% and 39.38%, respectively, while the rate in the NFIC siRNA group was 30%, 36.2% and 38.33% respectively, that was not significantly different. $P > 0.05$. (C) Results for the viability of hSCAPs after transfection with negative control or NFIC siRNAs, obtained by the colorimetric CCK-8 method, expressed as absorbance values, showed no significant difference in hSCAPs viability between the two groups. $P > 0.05$. (D) Flow cytometric analysis of cell cycle in hSCAPs at 48 h after transfection. (E) Real-time PCR analysis showed downregulated expression of *Cyclin E* and *Cyclin B1* in NFIC siRNA-transfected cells compared with control cells 24 h after transfection. $*P < 0.05$. (F) Representative images of wound-healing assays are shown. (G) The results reported as the numbers of cells moving into the wound showed no significant difference between the two groups. $P > 0.05$. (H) RT-PCR revealed that the expression levels of *DSPP* was decreased significantly in the *NFIC* siRNA group compared with the control group. Yet the expression of *DMP1* was increased significantly. Expression of *ALP*, *OCN* and *COLLA I* was not significantly changed 24 h after transfection. $*P < 0.05$, $**P < 0.01$. Scale bars 100 μm (A), 500 μm (F).

unknown. NFIC may work in the common molecular regulation mechanism sharing by the development and repair of dentin. Further research will be required to identify these different pathways at various stages of dentin formation and the relationship between the expression and function of NFIC.

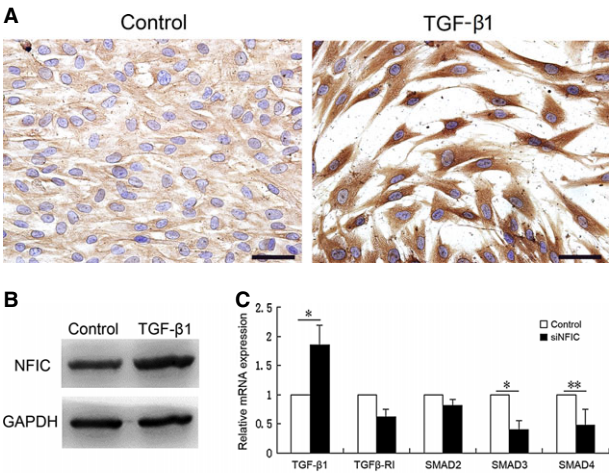

Fig. 6. The interaction of NFIC with TGF-β1. (A) Immunocytochemical staining and (B) Western blotting shows a higher level of NFIC expression in hSCAPs 24 h after TGF-β1 treatment. (C) Expression of *TGF-β1* is increased and *SMAD3*, *SMAD4* decreased significantly in the *NFIC* siRNA group compared with the control group 24 h after transfection. GAPDH was used as a loading control. $^{*}P < 0.05$ and $^{**}P < 0.01$. Scale bars 50 μm (A).

Nfic-deficient mice have been reported to have abnormal odontoblasts with a round shape, no odontoblastic processes and no polarity (16) and that ectomesenchymal cells near the abnormal root show no expression of *Dspp* mRNA. The odontoblasts of murine incisors exhibit a decreased level of DSP expression that is a product of a *Dspp*-a dentin-specific gene (17). In the present study, NFIC and DSP had consistent expression patterns: both increased at the early stage of the induced mineralization of hSCAPs, and decreased at the late stage. Based on these findings, we suggest that NFIC and DSPP are likely to have a more compact expression and functional relationship, and that NFIC may be another dentin-specific marker during odontoblast differentiation in humans. While the levels of NFIC and DSPP were decreased, the expression of mineralization related genes *ALP* and *OCN* increased gradually. ALP is important in physiological mineralization, which can hydrolyse the organophosphate and damage calcification inhibitors to start and accelerate mineralization (19). As a valid marker of osteoblast mineral deposition in vitro, OCN is expressed only in the matrix mineralization at the late phase of osteoblasts differentiation (20). Thus we presume that NFIC is involved not in the biomineralization of predentin but in the regulation of odontoblast differentiation.

The development of the dental root involves a complicated sequence of temporal and spatial events such as cell proliferation, migration and differentiation. To further work out the function of NFIC on this process, we used siRNA to selectively knock down NFIC expression in hSCAP and cultured in vitro. Our results showed that the knockdown of NFIC had no significant impact on the proliferation and migration of the cells and the regulation of NFIC focus more on the differentiation of hSCAPs. Dentin matrix protein 1 (DMP1) plays crucial roles in the formation of the mineralized tissues. The expression of DMP1 appears in dentin, bone and the odontoblasts newly formed, but decrease in odontoblasts entering the secretory phase. Previous studies have provided strong evidence that DMP1 might regulate the expression of DSPP during dentinogenesis. The expression of endogenous DSPP was remarkably reduced in the *Dmp1* KO mice. The transgenic expression of DSPP rescued the tooth and alveolar bone defects of the *Dmp1* KO mice. In contrast, the expression of DMP1 was not altered in the *Dspp* KO mice (21). Our analyses showing that the expression of DSPP was inhibited and DMP1 was promoted significantly after NFIC knockdown, indicate that DSPP might be putative downstream effector molecule of NFIC that could mediate the interaction of DMP1 and DSPP in human dentinogenesis. Furthermore, we also found that NFIC knockdown did not affect the expression of *ALP*, *OCN* and *COLLA I*, supporting the view above that NFIC is not necessary for dentin mineralization in the root.

The TGF-β family consists of growth factors that have wide-ranging functions in development and tissue homeostasis. TGF-β1 initiates cellular actions by recruiting and phosphorylating the cell-surface TGF-β-RI upon binding to TGF-β-RII. Activated TGF-β-RI then phosphorylates the cytoplasmic proteins SMAD2 and SMAD3, thereby enabling their to binding to the common downstream signal SMAD4 to form a SMAD-complex that translocates to the nucleus to regulate transcription of specific genes (22, 23). *Nfic*-deficient mice have higher levels of TGF-β-R1 and p-Smad2/3 in the odontoblasts and pulp cells of their incisors (11). Recent studies also showed that TGF-β/BMP signaling relies on a Smad4-dependent mechanism in regulating *Nfic* expression via SHH signaling to control murine root development (24). Those results imply that a functional relationship between NFIC and TGF-β1 signaling is present, but how NFIC regulates TGF-β1 is not known. Exposure of cells to TGF-β1 can trigger various cellular responses: differentiation, arrest of cell growth and apoptosis. In the present study, TGF-β1 stimulation in vitro upregulated the expression of NFIC proteins. Conversely, inactivation of *NFIC* by siRNA knockdown could promote expression of *TGF-β1* and inhibit expression of *SMAD3* and *SMAD4*. We speculate that the increased expression of *TGF-β1* reflects compensation of the inhibition of its downstream molecules *SMAD3* and *SMAD4* by *NFIC* knockdown. A report that Smad3 binds to NFIC through its MH1 domain (25) also provides evidence supporting our data. Our data suggest that TGF-β1 has a positive regulatory role for NFIC, whereas NFIC has a negative regulatory effect on TGF-β1 expression through *SMAD3* and *SMAD4*, and that a complex signaling cycle is thereby formed. Thus, NFIC may regulate odontoblast differentiation in hSCAPs through TGF-β signaling pathways. The specific functional relationship of these molecules in regulating root development needs further investigation.

The effect of NFIC knockdown on the cell cycle of hSCAPs was also studied. The results suggest that NFIC knockdown leads to G1-phase arrest of hSCAPs by downragulating the G1-phase-related genes Cyclin E and that NFIC may participate in regulating cell cycle progression. In addition the expression of G2-phase-related genes Cyclin B1 (26) was also decreased. However G2 and M phase cannot be distinguished by flow cytometry, and cell cycle involves many regulatory factors, so the effect of NFIC on cell cycle still need further study.

In conclusion, we propose that NFIC is involved in the regulation of differentiation of hSCAPs into odontoblasts during root development in young permanent teeth in a stage- and tissue-specific manner. This phenomenon could be regarded as a marker of odontoblast differentiation. NFIC had no essential impact on the proliferation and migration of hSCAPs, but focus the function on regulating odontoblastic differentiation of hSCAPs through TGF-β1 and DMP1-DSPP signaling pathways. From a clinical perspective, this study based on human stem cells leading to more practical results. However owing to the numerous regulatory factors in root development in vivo, there are some limitations with our data. Further in vivo studies are required to confirm this conclusion.

Acknowledgements – This work was supported by the National Natural Science Foundation of China (nos 81170928 and 81141011).

Conflicts of interest – No competing financial interests exist.

References

1. Nagata K, Guggenheimer RA, Enomoto T, Lichy JH, Hurwitz J. Adenovirus DNA replication in vitro identification of a host factor that stimulates synthesis of the preternal protein-dCMP complex. *Proc Natl Acad Sci* 1982; **79**: 6438–6442.
2. Gronostajski RM. Roles of the NFI/CTF gene family in transcription and development. *Gene* 2000; **249**: 31–45.
3. Shu T, Butz KG, Plachez C, Gronostajski RM, Richards LJ. Abnormal development of forebrain midline glia and commissural projections in Nfia knock-out mice. *J Neurosci* 2003; **23**: 203–212.
4. Steele-Perkins G, Plachez C, Butz KG, Yang G, Bachurski CJ, Kinsman SL, Litwack ED, Richards LJ, Gronostajski RM. The transcription factor gene *Nfib* is essential for both lung maturation and brain development. *Mol Cell Biol* 2005; **25**: 685–698.
5. Gründer A, Ebel TT, Mallo M, Schwarzkopf G, Shimizu T, Sippel AE, Schrewe H. Nuclear factor I-B (*Nfib*) deficient mice have severe lung hypoplasia. *Mech Dev* 2002; **112**: 69–77.
6. Driller K, Pagenstecher A, Uhl M, Omran H, Berlis A, Gründer A, Sippel AE. Nuclear factor I X deficiency causes brain malformation and severe skeletal defects. *Mol Cell Biol* 2007; **27**: 3855–3867.
7. Steele-Perkins G, Butz KG, Lyons GE, Zeichner-David M, Kim HJ, Cho MI, Gronostajski RM. Essential role for NFI-C/CTF transcription replication factor in tooth root development. *Mol Cell Biol* 2003; **23**: 1075–1084.
8. Xing X, Deng Z, Yang F, Watanabe S, Wen L, Jin Y. Determination of genes involved in the early process of molar root development initiation in rat by modified subtractive hybridization. *Biochem Biophys Res Commun* 2007; **363**: 994–1000.
9. Massagué J. How cells read TGF-β signals. *Nat Rev Mol Cell Biol* 2000; **1**: 169–178.
10. Smith AJ, Matthews JB, Hall RC. Transforming growth factor-beta1 (TGF-beta1) in dentine matrix. Ligand activation and receptor expression. *Eur J Oral Sci* 1998; **106** (Suppl): 179–184.
11. Lee DS, Park JT, Kim HM, Ko JS, Son HH, Gronostajski RM, Cho MI, Choung PH, Park JC. Nuclear factor I-C is essential for odontogenic cell proliferation and odontoblasted differentiation during tooth root development. *J Biol Chem* 2009; **254**: 17293–17303.
12. Thyagarajan T, Sreenath T, Cho A, Wright JT, Kulkarni AB. Reduced expression of dentin sialophosphoprotein is associated with dysplastic dentin in mice overexpressing transforming growth factor-beta 1 in teeth. *J Biol Chem* 2001; **276**: 11016–11020.
13. Seo BM, Miura M, Gronthos S, Bartold PM, Batouli S, Brahim J, Young M, Robey PG, Wang CY, Shi S. Investigation of multipotent postnatal stem cells from human periodontal ligament. *Lancet* 2004; **364**: 149–155.
14. Kim MY, Reyna J, Chen LS, Zeichner-David M. Role of the transcription factor NFIC in odontoblast gene expression. *J Calif Dent Assoc* 2009; **37**: 875–881.
15. Lee DS, Yoon WJ, Cho ES, Kim HJ, Gronostajski RM, Cho MI, Park JC. Crosstalk between nuclear factor I-C and transforming growth factor-β1 signaling regulates odontoblast differentiation and homeostasis. *PLoS ONE* 2011; **6**: e29160.
16. Lee TY, Lee DS, Kim HM, Ko JS, Gronostajski RM, Cho MI, Son HH, Park JC. Disruption of Nfic causes dissociation of odontoblasts by interfering with the formation of intercellular junctions and aberrant odontoblast differentiation. *J Histochem Cytochem* 2009; **57**: 469–476.
17. Park JC, Herr Y, Kim HJ, Gronostajski RM, Cho MI. Nfic gene disruption inhibits differentiation of odontoblasts responsible for root formation and results in formation of short and abnormal roots in mice. *J Periodontol* 2007; **78**: 1795–1802.
18. Xu L, Tang L, Jin F, Liu XH, Yu JH, Wu JJ, Yang ZH, Wang YX, Duan YZ, Jin Y. The apical region of developing tooth root constitutes a complex and maintains the ability to generate root and periodontium-like tissues. *J Periodontal Res* 2009; **44**: 275–282.
19. Register TC, McLean FM, Low MG, Wuthier RE. Roles of alkaline phosphatase and labile internal mineral in matrix vesicle-mediated calcification. *J Biol Chem* 1986; **261**: 9534.
20. Neve A, Corrado A, Cantatore FP. Osteocalcin: skeletal and extra-skeletal effects. *J Cell Physiol* 2013; **228**: 1149–1153.
21. Gibson MP, Zhu Q, Wang S, Liu Q, Liu Y, Wang X, Yuan B, Ruest LB, Feng JQ, D'Souza RN, Qin C, Lu Y. The rescue of dentin matrix protein 1 (DMP1)-deficient tooth defects by the transgenic expression of dentin sialophosphoprotein (DSPP) indicates that DSPP is a downstream effector molecule of DMP1 in dentinogenesis. *J Biol Chem* 2013; **288**: 7204–7214.
22. Massague J, Wotton D. Transcriptional control by the TGF-beta/Smad signaling system. *EMBO J* 2000; **19**: 1745–1754.
23. Hill CS. Nucleocytoplasmic shuttling of Smad proteins. *Cell Res* 2009; **19**: 36–46.
24. Huang X, Xu X, Bringas P Jr, Hung YP, Chai Y. Smad4-Shh-Nfic signaling caseade-mediated epithelial-mesenehymal interaction is crucial in regulating tooth root development. *J Bone Miner Res* 2010; **25**: 1161–1178.
25. Luciakova K, Kollarovic G, Barath P, Nelson BD. Growth-dependent repression of human adenine nucleotide translocator-2 (ANT2) transcription: evidence for the participation of Smad and Sp family proteins in the NF1-dependent repressor complex. *Biochem J* 2008; **412**: 123–130.
26. Pagliuca FW, Collins MO, Lichawska A, Zegerman P, Choudhary JS, Pines J. Quantitative proteomics reveals the basis for the biochemical specificity of the cell-cycle machinery. *Mol Cell* 2011; **43**: 406–417.